ChemBioChem

Research Article
doi.org/10.1002/cbic.202200407

Chemistry Europe
European Chemical Societies Publishing

www.chembiochem.org

VIP *Very Important Paper*

Chemoselective Labeling and Immobilization of Phosphopeptides with Phosphorimidazolide Reagents

Nathaniel W. Brown[+,[a, c]] Sandra K. Schlomach[+,[a, b]] Alan M. Marmelstein,[[a, c]] and Dorothea Fiedler*[[a, b]]

Protein phosphorylation is one of the most ubiquitous post-translational modifications, regulating numerous essential processes in cells. Accordingly, the large-scale annotation of phosphorylation sites continues to provide central insight into the regulation of signaling networks. The global analysis of the phosphoproteome typically relies on mass spectrometry analysis of phosphopeptides, with an enrichment step necessary due to the sub-stoichiometric nature of phosphorylation. Several affinity-based methods and chemical modification strategies have been developed to date, but the choice of enrichment method can have a considerable impact on the results. Here, we show that a biotinylated, photo-cleavable phosphorimidazolide reagent permits the immobilization and subsequent cleavage of phosphopeptides. The method is capable of the capture and release of phosphopeptides of varying characteristics, and this mild and selective strategy expands the current repertoire for phosphopeptide chemical modification with the potential to enrich and identify new phosphorylation sites in the future.

Introduction

Reversible protein phosphorylation is an important post-translational modification (PTM), regulating a variety of essential processes in cells such as DNA repair, cell growth, and cell metabolism.[1–3] As such, new insights into the regulation of cell signaling in healthy and diseased states can be gained by investigating the phosphoproteome. Accordingly, the study of protein phosphorylation has remained squarely in focus over the past decades. The global interrogation of protein phosphorylation typically relies on mass spectrometry (MS) analysis of phosphopeptides (pPeps) generated by a proteolytic digestion of the proteome of interest.[4] Due to the sub-stoichiometric nature of phosphorylation, enrichment of phosphorylated peptides over non-phosphorylated peptides is of critical importance. Strategies developed to address this need generally fall into two categories: affinity enrichment or chemical modification.[5–9] For affinity enrichment, antibodies have been applied for immunoprecipitation of specific phosphoproteins or phosphopeptides of interest.[10–12] However, robust and reliable pan-specific antibodies are only available for phosphotyrosine, phosphohistidine and phosphoarginine,[5,6,13–16] which are less abundant than phosphoserine and phosphothreonine.

Therefore, affinity-based enrichment is generally achieved through immobilized metal-ion affinity chromatography (IMAC) or metal-oxide affinity chromatography (MOAC).[7–9] The metal-based affinity methods are well-suited for global analyses and are by far the most popular choices for proteome-wide studies of phosphoregulation,[3,17–20] but special precautions are necessary to minimize non-specific binding of acidic amino acid side chains, while harsh acidic and basic conditions exclude the identification of more labile amino acid phosphorylation sites.[5,17,21]

Chemical modification strategies exploit the unique chemistry of the phosphoryl group to modify phosphopeptides for subsequent enrichment and identification (Figure 1). One such method is β-elimination of phosphoric acid (Figure 1a), induced by barium hydroxide, followed by Michael addition (BEMA), introduced by the Chait laboratory in 2001.[22] Tagging of the generated Michael acceptors by the addition of a nucleophile facilitates the subsequent identification of phosphosites,[22–31] but is not suitable for studying tyrosine phosphorylation. Pflum and co-workers introduced a biochemical tagging method (Figure 1b), where ATP-biotin was incubated with various peptide and protein substrates of mammalian kinases, establishing a broad substrate scope for individual kinase substrates and utilizing endogenous kinases to label phosphoproteins in HeLa cell lysates.[32,33] Another chemical derivatization strategy developed by the Aebersold laboratory relies on phosphoramidate chemistry (PAC, Figure 1c), in which a phosphoramidate bond is formed between the phosphoryl group of a phosphopeptide and an amino group of a solid

[a] *Dr. N. W. Brown,[+] S. K. Schlomach,[+] Dr. A. M. Marmelstein, Prof. Dr. D. Fiedler*
Department of Chemical Biology
Leibniz Forschungsinstitut für Molekulare Pharmakologie (FMP)
Robert-Rössle-Str. 10, 13125 Berlin (Germany)
E-mail: fiedler@fmp-berlin.de
[b] *S. K. Schlomach,[+] Prof. Dr. D. Fiedler*
Department of Chemistry
Humboldt-Universität zu Berlin
Brook-Taylor-Straße 2, 12489 Berlin (Germany)
[c] *Dr. N. W. Brown,[+] Dr. A. M. Marmelstein*
Department of Chemistry, Princeton University
Washington Rd., Princeton, NJ 08544 (USA)
[+] *These authors contributed equally to this work.*

Supporting information for this article is available on the WWW under https://doi.org/10.1002/cbic.202200407

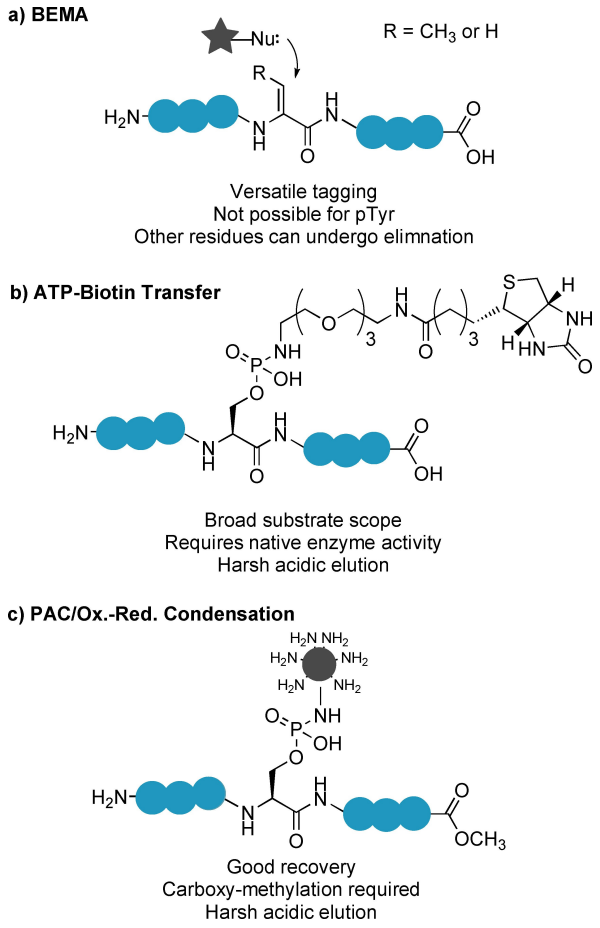

Figure 1. Current methods for phosphopeptide enrichment relying on chemical derivatization.

phase.[34–36] PAC enrichment of a standard phosphopeptide from a bovine serum albumin (BSA) background resulted in ~40% recovery, and in a separate experiment was able to identify 571 unique phosphorylation sites in *Drosophila melanogaster* lysates.[36] The Pflum laboratory also developed an oxidation-reduction condensation method which forms a phosphoramidate bond similarly to PAC.[37] This method recovered phosphopeptides in the presence of non-phosphorylated peptides and was able to capture and release whole phosphoproteins.[37]

Depending on the choice of enrichment protocol, distinct subsets of the phosphoproteome are detected.[38–40] As such, there is a need to explore alternative, complementary phosphopepetide enrichment methods that could potentially uncover additional features of the phosphoproteome.

Phosphorimidazolide reagents react selectively with phosphoryl groups,[41,42] requiring only a divalent metal cation and polar organic solvent for efficient phosphoanhydride bond formation.[43–46] Our laboratory demonstrated that phosphorimidazolide reagents are capable of selectively converting phosphorylated residues of phosphopeptides and phosphoproteins into phosphoanhydrides, even in the presence of numerous nucleophilic amino acid side-chains.[47,48] A biotinylated, photocleavable phosphorimidazolide (btNPE-imidazolide (**1**), Figure 2a) reacted selectively with phosphoproteins and purification was achieved *via* a sequence of immobilization, followed by photoirradiation.[48] Here, we apply the biotinylated, photocleavable reagent in the development of a novel phosphopeptide enrichment strategy: chemoselective labeling and immobilization of phosphopeptides with phosphorimidazolide reagents, termed CLIPP (Figure 2b). We show that **1** permits the capture and release of phosphopeptides of varying characteristics, including acidic, basic, hydrophobic, mono- or di-phosphorylated phosphopeptides, and even a phosphotyrosine-containing peptide. We also demonstrate for the first time that lanthanide(III) ions are able to hydrolyze pyrophosphate monoesters at mild temperature and pH. The ability to modify and elute a diverse set of phosphopeptides under mild conditions positions CLIPP well for future use in global phosphoproteomic enrichment experiments.

Results and Discussion

Derivatization, immobilization, and elution of a model phosphopeptide

The btNPE-imidazolide (**1**) contains functionalities for both immobilization (biotin moiety "bt") and elution (photolabile "NPE" (1-(2-nitrophenyl)ethyl) linker). These attributes make **1** well-suited for the selective enrichment of phosphopeptides. A workflow was envisioned that would allow the selective modification of phosphopeptides by **1** for affinity purification followed by photoirradiation to elute free pyrophosphopeptides

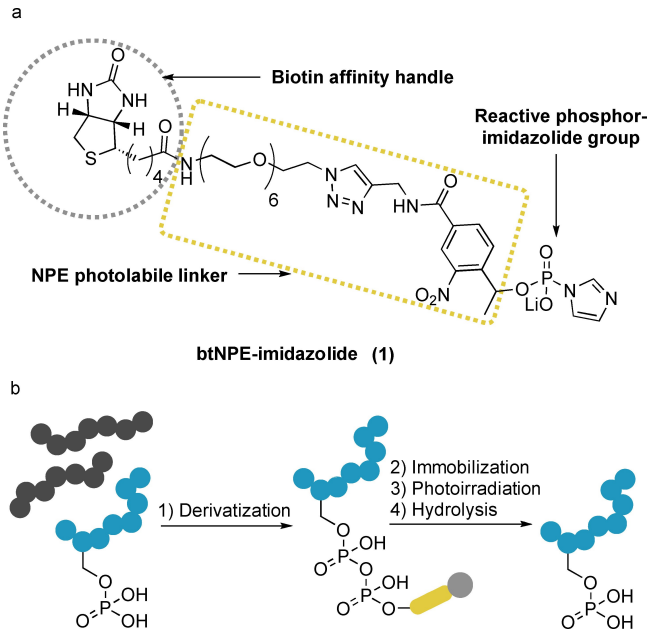

Figure 2. (a) Photocleavable phosphorimidazolide (btNPE-imidazolide (**1**)) contains both a biotin (bt) affinity handle and a photocleavable nitrophenylethyl (NPE) linker. (b) Generic CLIPP workflow for phosphopeptide enrichment. Phosphopeptides are selectively pyrophosphorylated, immobilized, eluted, and hydrolyzed to re-generate the native phosphopeptides.

(ppPeps), and mild hydrolysis to regenerate the original pPep for identification (Figure 2b). To explore the utility of **1** for such a workflow, a model phosphoserine-containing phosphopeptide (**pSer-2**) was synthesized by solid-phase peptide synthesis (SPPS) to test every step of the workflow individually. Reagent **1** reacted with **pSer-2** in the presence of Zn^{2+} cations, to furnish **btNPE-ppSer-2** as measured by high performance liquid chromatography (HPLC). Pyrophosphorylation conditions mirrored those that had been already established[47] with a 9:1 mixture of dimethylacetamide (DMA) to water (DMA:H_2O) providing quantitative conversion (see Experimental Section, Figure 3).

We then assessed the immobilization and subsequent elution of **ppSer-2** (Figure 3). Immobilization of **btNPE-ppSer-2** using a streptavidin agarose resin proved to be quantitative, as measured by the disappearance of peptide in the supernatant *via* HPLC. To cleave the photolabile linker and release **ppSer-2**, resin-bound **btNPE-ppSer-2** was irradiated at 360 nm for 1 hour with vigorous stirring. HPLC absorbance indicated the presence of **ppSer-2** in the supernatant (**Figure 3**), and this confirmation of proof of concept allowed us to proceed to the final step of the workflow: pyrophosphopeptide hydrolysis.

Lanthanide ions promote mild hydrolysis of pyrophosphopeptide

Pyrophosphopeptides such as **ppSer-2** exhibit poorer ionization and chromatographic properties than phosphopeptides,[49] therefore a final step to hydrolyze the phosphoanhydride bond to regenerate **pSer-2** was preferable. Lanthanide ions have been known for many years to be capable of mediating the hydrolysis of phosphodiester bonds of oligonucleotides under mild conditions.[50–53] This hydrolytic activity could potentially be translated to the hydrolysis of the phosphoanhydride bond in **ppSer-2**.[48] Following chemical synthesis of **ppSer-2** (Scheme S1), three different commercially available lanthanide(III) triflate salts were assessed for their hydrolytic activity: lutetium(III) (Lu^{3+}), yttrium(III) (Y^{3+}), and lanthanum(III) (La^{3+}). Reactions were conducted in 20 mM HEPES buffer at pH 7.8 to maintain a near-neutral environment. **ppSer-2** was then subjected to incubation for 18 h at 25, 37 (Table 1), or 50 °C (Table S1) in the presence of 0, 1, 2, or 5 molar equivalents of the different lanthanide ions. While incubation of **ppSer-2** in buffer alone resulted in no observable hydrolysis (Table 1, entries 1 & 2), the addition of lanthanide ions triggered conversion to **pSer-2**. One molar equivalent of Lu^{3+} or Y^{3+} ions produced near-quantitative conversion at 37 °C (Table 1, entries 7, 9, 11, 13), while La^{3+} ions generally proved inadequate for complete hydrolysis (Table 1, entries 3–6). At higher temperature and greater lanthanide excess, the yield of **pSer-2** appeared to decrease (Table 1, Table S1). Instead, we observed the formation of a side product displaying the loss of phosphoric acid, suggesting β-elimination of phosphoserine to dehydroalanine (Figure S1). Two molar equivalents of lanthanide ions in a ratio of 1:1 Lu^{3+}/Y^{3+} at 37 °C for 18 h provided 89% conversion to the desired product and was chosen as the standard hydrolysis condition moving forward (Table 1, entry 18). While other entries provided a greater yield (Table 1, entries 9, 13, 14, 17), applying two total molar equivalents ensured a high yield of **pSer-2**. Furthermore, the mixture of lanthanide ions guards against potential variations in the hydrolytic potential of either metal for any given pyrophosphopeptide, as was observed with lanthanum.

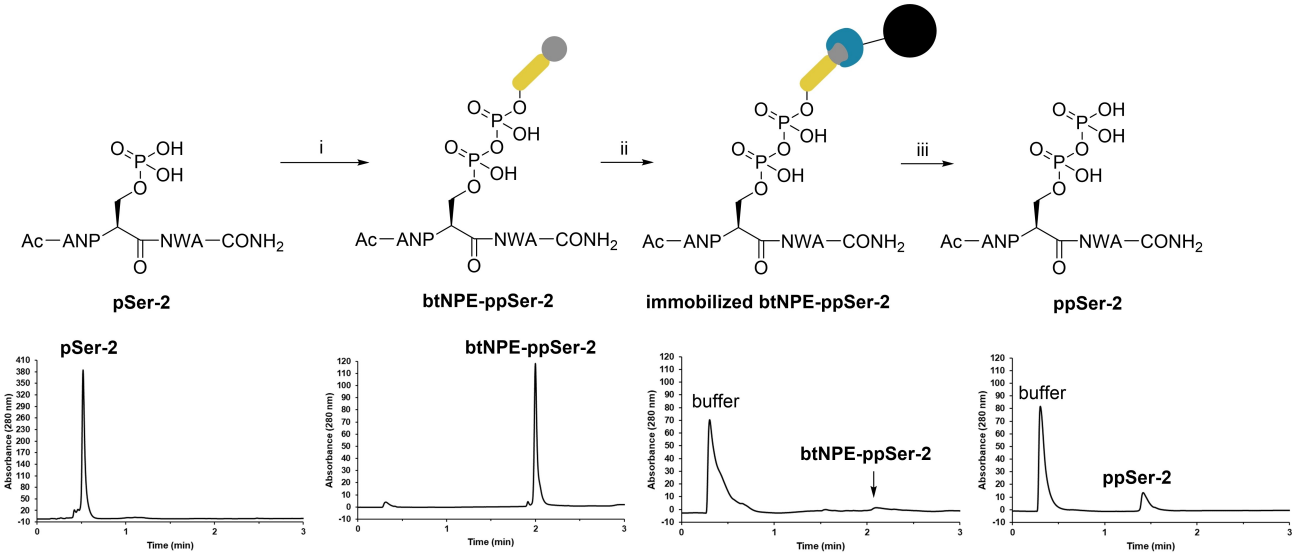

Figure 3. Top: Pyrophosphorylation of **pSer-2** with **1** to furnish **btNPE-ppSer-2**, followed by immobilization onto streptavidin resin (blue element and black sphere) and elution of **ppSer-2** after photoirradiation. Bottom: Representative absorbance traces after each step are shown below for retention time reference and proof of principle. Progress of steps 1–3 followed *via* LC–MS absorbance at 280 nm. Note that each peptide exhibits different absorbance at 280 nm, so peak intensities are not directly comparable. Y-axes adjusted for clarity of presentation. Conditions: (i) 3 eq. **1**, 8 eq. $ZnCl_2$; 9:1 DMA/$H_2$0, 45 °C, 3 h (ii) GE Sepharose High Performance Streptavidin Resin (300 nmol/mL); 20 mM phosphate, 150 mM NaCl, pH 7.5, r.t., 30 min. (iii) 360 nm photoirradiation; 20 mM HEPES, pH 7.8, r.t., 1 h.

Table 1. Lanthanide hydrolysis of **ppSer-2**. **ppSer-2** was incubated for 18 h at 25 or 37 °C with or without the presence of the indicated Ln^{3+} triflate salt at 1 or 2 molar equivalents. Percent yield **pSer-2** calculated *via* HPLC standard curve (see Experimental Section for more detail).

Entry	Ln^{3+}	T [°C]	Ln^{3+} eq.	% yield **pSer-2**
1	None	25	0	4
2		37	0	5
3	La^{3+}	25	1	8
4			2	17
5		37	1	23
6			2	43
7	Lu^{3+}	25	1	59
8			2	49
9		37	1	>95
10			2	88
11	Y^{3+}	25	1	24
12			2	44
13		37	1	95
14			2	>95
15	1:1 Lu^{3+}/Y^{3+}	25	1	42
16			2	47
17		37	1	>95
18			2	89

Given the success of the lanthanide mediated hydrolysis of **ppSer-2**, we wondered whether one step of the workflow could be eliminated, by directly eluting **pSer-2** from the solid-phase resin *via* lanthanide-mediated hydrolysis on the beads. To explore this possibility, **btNPE-ppSer-2** was immobilized onto streptavidin resin and subsequently subjected directly to lanthanide hydrolysis under different conditions. Unfortunately, even at 50 °C in the presence of up to 10 molar equivalents of lanthanide (Table S2), only 13% of **pSer-2** was eluted. While keeping the number of workflow steps to a minimum was desirable, the success of the solution-phase hydrolysis compelled us to continue eluting pyrophosphopeptides from the resin *via* photoirradiation.

Full workflow for phosphopeptide enrichment

With each step of the proposed procedure characterized and validated, a full workflow was conducted in which **pSer-2** was sequentially pyrophosphorylated with **1**, immobilized on streptavidin resin, eluted by photoirradiation, and finally hydrolyzed with lanthanide ions to recover **pSer-2** (Figure 4). While 1.5 h provided complete conversion of **pSer-2** to **btNPE-ppSer-2**, the pyrophosphorylation reaction was conducted over 3 h to ensure maximum conversion. When 17.5 nmol of phosphopeptide **pSer-2** were subjected to the entire workflow, the overall recovery after lanthanide hydrolysis amounted to 66±2% (triplicate, as calculated by HPLC peak area of the quenched hydrolysis reaction). Increasing the photoirradiation time to 3 h did not improve the recovery of **pSer-2** (Figure S2). Conversely, we also decided to test shorter irradiation times for immobilized **btNPE-ppSer-2** to identify any potential photo-mediated degradation that could reduce the elution yields. Irradiation for 15 minutes compared to 1 h resulted in a lower elution yield, while 30 minutes irradiation time resulted in similar yields of **ppSer-2** compared to 1 hour (Figure S3), indicating that 1 hour of irradiation was not adversely impacting the overall yield. Although a higher yield was expected given the success of each individual step of the work-flow, a yield of 66% for this multi-step workflow is a promising result.

Validation of CLIPP with diverse peptides

While **pSer-2** was successfully modified and released *via* the CLIPP workflow, it is an unremarkable synthetic peptide with a protected N- and C-terminus. To better understand the efficacy of the CLIPP workflow on biologically relevant substrates, a panel of 4 tryptic phosphopeptides was synthesized, all of which were previously identified in different published phosphoproteomics experiments (Figure 4a): a phosphotyrosine-containing peptide derived from cyclin-dependent kinase 2 (**pTyr-CDK2** (**pTyr-3**));[54] a basic phosphoserine-containing peptide from myristoylated alanine-rich casein kinase substrate protein (**pSer-MARCKS** (**pSer-4**)) along with its doubly phosphorylated analog ((**pSer)$_2$-MARCKS** ((**pSer)$_2$-5**));[55] and an acidic phosphoserine-containing peptide from β-casein (**pSer-βCasein** (**pSer-6**)), used previously to validate the PAC phosphopeptide enrichment platform.[35] Together, the selected peptides encompassed acidic, basic, and hydrophobic characteristics. **pTyr-3** possessed a phosphotyrosine residue, while the synthesis of the bis-phosphorylated **(pSer)$_2$-5** allowed the ability to assess any potential bias between mono- and bis-phosphorylated peptides, as has been observed for IMAC and MOAC enrichment procedures.[6,8]

pTyr-3 and **pSer-4** were first subjected (separately) to the CLIPP workflow established for **pSer-2**. However, despite the success of **pSer-2** the yields were much lower for **pTyr-3** and **pSer-4** (34% and 21%, respectively, Figure 4a). Since **pTyr-3** and **pSer-4** are more representative of native phosphopeptides found in phosphoproteomics experiments compared to **pSer-2**, we returned to optimize the workflow to improve the overall recovery of **pTyr-3** and **pSer-4**. To do so, we repeated the full enrichment workflow with each peptide (**pSer-2**, **pTyr-3**, **pSer-4**), and removed aliquots for HPLC analysis after each step: streptavidin bead immobilization, to check for unreacted phosphopeptide; photoirradiation, to check for photocleavage yield; and lanthanide hydrolysis, to check for overall yield/hydrolysis efficiency (Figure 4b). HPLC standard curves were used for the quantification of **pSer-2**, **pTyr-3**, and **pSer-4**, biotinylated ppPeps **btNPE-ppSer-2**, **btNPE-ppTyr-3**, and **btNPE-ppSer-4**, and free ppPeps **ppSer-2**, **ppTyr-3**, and **ppSer-4** (see Supporting Information and Scheme S1).

As summarized in Figure 4b, the individual steps left room for improvement, so we started our optimization with the photoirradiation step. Purified **btNPE-ppSer-2**, **btNPE-ppTyr-3**, and **btNPE-ppSer-4** were each immobilized on streptavidin resin and irradiated at 360 nm for 1 h to elute **ppSer-2**, **ppTyr-3**, and **ppSer-4**. ppPeps in the supernatant were then quantified by HPLC (Figure 4c). The previously established photoirradiation conditions (Figure 3) afforded yields of 68%, 94%, and 80% for elution of **ppSer-2**, **ppTyr-3**, and **ppSer-4**, indicating that the

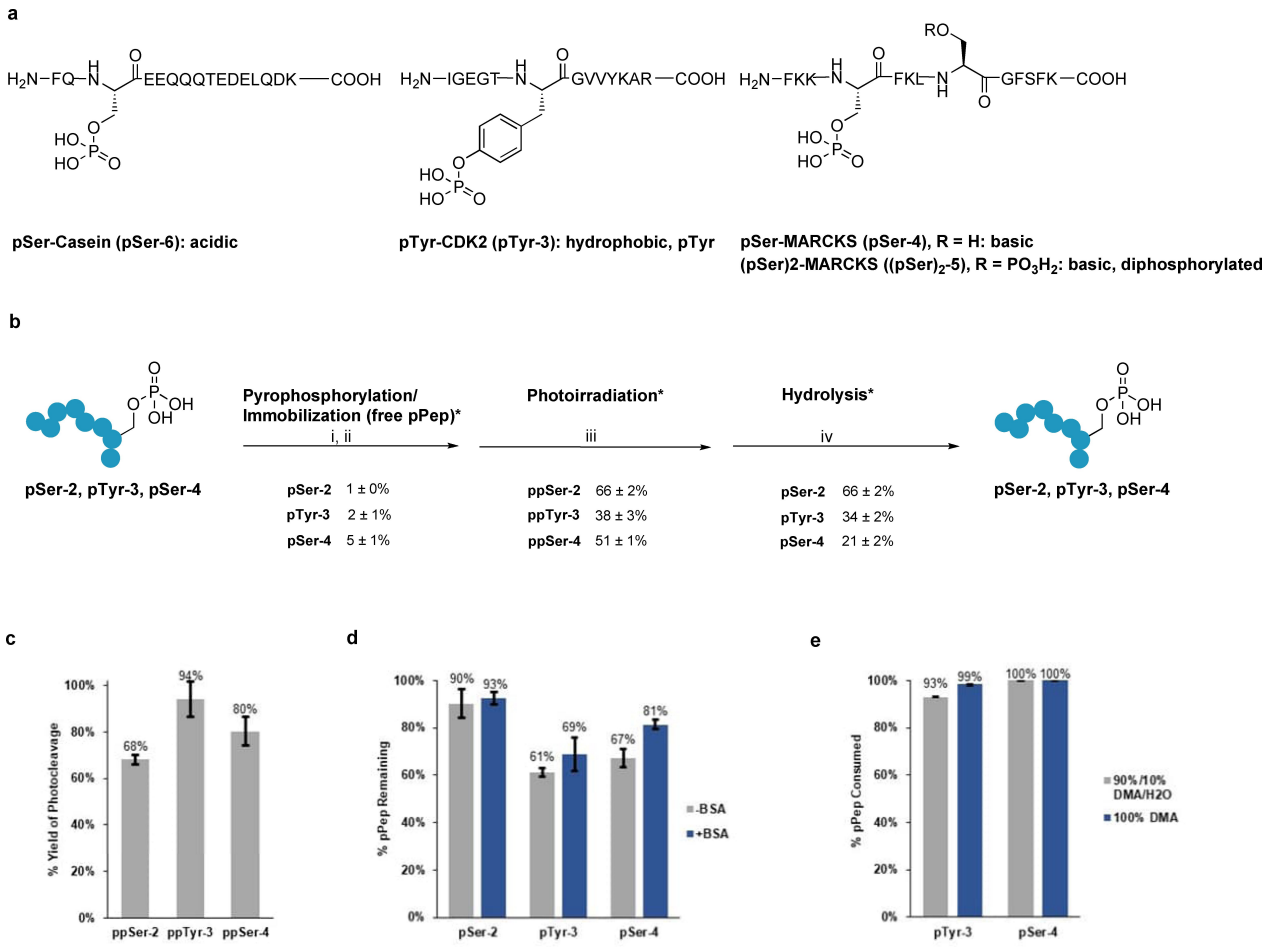

Figure 4. (a) Native phosphopeptides synthesized and used to evaluate scope of CLIPP workflow. (b) CLIPP workflow applied to model **pSer-2** as well as biologically relevant **pTyr-3** and **pSer-4**. Percentages and yields are expressed as relative to the amount of phosphopeptide at the beginning of the workflow following each step indicated. Equivalents are calculated relative to phosphoryl groups present on the peptide. Reaction conditions: i) 3 eq. **1**, 8 eq. $ZnCl_2$, 3 h, 45 °C, 9:1 DMA:H_2O ii) Streptavidin resin, 20 mM PBS pH 7.5, 30 min, r.t. iii) hν = 360 nm, 1 h, 20 mM HEPES pH 7.8 iv) 6 eq. 1:1 Lu^{3+}/Y^{3+}, 18 h, 37 °C, 20 mM HEPES pH 7.8. * Yields calculated following all steps in workflow up to and including indicated step (i.e. hydrolysis yield represents the overall yield of the full workflow). (c) Photocleavage yield of **btNPE-ppSer-2**, **btNPE-ppTyr-3**, and **btNPE-ppSer-4** immobilized onto streptavidin resin. Quantified by the amount of **ppSer-2**, **ppTyr-3**, and **ppSer-4** in supernatant following photoirradiation. (d) Quantification of pPeps **pSer-2**, **pTyr-3**, and **pSer-4** non-specific binding to streptavidin resin following 30 min incubation of 25 nmol pPep with 75 nmol streptavidin resin in 250 μL 1× PBS pH 7.5 containing 200 nmol $ZnCl_2$, 60 mM EDTA, 1.8% DMA. (e) Conversion of **pTyr-3**, **pSer-4** to **bt-NPE-ppTyr-3**, **btNPE-ppSer-4** following reaction of 25 nmol pPep with 75 nmol **1**, 200 nmol $ZnCl_2$ in 5 μL 9:1 DMA: H_2O or 100% DMA. Percent conversion measured by consumption of pPep. Errors are represented as the standard deviation of duplicate or triplicate trials, depending on availability of peptides and reagents.

lower overall recoveries for **pTyr-3** and **pSer-4** were not solely a result of reduced photocleavage efficiency or non-specific binding of ppPeps to the streptavidin resin.

The next possibility we investigated was whether unreacted phosphopeptide was binding non-specifically to the streptavidin resin following quenching of the pyrophosphorylation reaction. To probe this possibility, **pSer-2**, **pTyr-3**, and **pSer-4** were applied for 30 min to streptavidin resin under conditions identical to the quenched pyrophosphorylation reaction (see Experimental Section). As shown in Figure 4d, in each case a significant amount of phosphopeptide was retained by the streptavidin resin, which could be slightly improved upon pre-blocking the streptavidin resin with 1.0–1.5 mg/mL BSA. These results indicate that a significant fraction of pPeps may remain unreacted in the first step, and instead binds the resin non-specifically, which explains why it was not detected in the immobilization supernatant earlier (Figure 3, 4b). This then prompted an investigation of the pyrophosphorylation reaction conditions. Initially, the reaction was conducted in 9:1 DMA: H_2O, however, previous studies have shown that increasing the water present in the reaction leads to depressed reaction rates and lower overall conversion.[47,48] To test if this was the cause of reduced conversion, 25 nmol of **pTyr-3** and **pSer-4** were each reacted with 3 eq. (75 nmol) of **1** and 8 eq. of $ZnCl_2$ in either 100% DMA or 9:1 DMA:H_2O. Following incubation at 45 °C for 3 h, the reaction was quenched and phosphopeptide consumption analyzed by HPLC to quantify conversion (Figure 4e). The improvement in conversion for **pTyr-3** in 100% DMA suggested to us that an incomplete pyrophosphorylation reaction in 9:1 DMA:H_2O could be resulting in lower overall

yields. While prior studies on a benzylated phosphorimidazolide reagent had indicated broad stability under pyrophosphorylation conditions in 1:1 and 9:1 DMA:H_2O,[48] we also considered that reagent **1** could be breaking down under the reaction conditions, resulting in a lower apparent yield of pyrophosphopeptide. To check for the stability of btNPE-imidazolide (**1**), the reagent was incubated under the optimized reaction conditions (100% DMA, 45 °C, 2.67 eq. $ZnCl_2$), and the mixture was monitored *via* ^{31}P NMR over approximately 20 h. The data indicate that reagent **1** is stable over the course of the pyrophosphorylation reaction, with only 10% degradation present after 3 h, and 26% after ca. 19 h (Figure S4). As such, the pyrophosphorylation reaction conditions were not adjusted further. The workflow from Figure 4b was then amended to include pyrophosphorylation in 100% DMA to ensure greater conversion of phosphopeptide, and pre-treatment of streptavidin resin with 1.5 mg/mL BSA to reduce non-specific binding of any unreacted phosphopeptide to the resin prior to photoirradiation. **pSer-2**, **pTyr-3**, and **pSer-4** were then submitted to the new workflow (Table 2, column II) which resulted in a 4%, 16% and 8% improvement in overall yield, respectively. Peptides **pSer-6** and **$(pSer)_2$-5** were then submitted to the optimized workflow, furnishing recovery yields of 12% and 38%, respectively (Table 2, column II). While there is variability between different peptides, we observed a general ability to recover peptides of differing characteristics, including a phosphotyrosine-containing peptide (**pTyr-3**) suggest potential broad compatibility with native phosphopeptides.

To probe possible biases CLIPP may demonstrate towards certain peptide sequences, equimolar quantities of peptides **pTyr-3**, **pSer-4**, **$(pSer)_2$-5** and **pSer-6** were mixed together, and the mixture was subjected to the CLIPP workflow. Following hydrolysis, the mixture was analyzed by LC–MS/MS, and all four pPeps were quantified by the integrated area of their most abundant extracted ions as compared to a standard mixture (Figure S5). While all peptides were present, there was some variation in yield (Table 2, Column III).

In particular, **pSer-4** and **$(pSer)_2$-5**, both containing a large number of basic amino acid residues, showed a drastic decrease in enrichment yield, while phosphotyrosine-containing **pTyr-3** demonstrated a moderate decrease in yield (less than 2-fold reduction) and **pSer-6** recovery yield increased nearly 2-fold, from 12% to 18%. Applying the CLIPP workflow to a mixture of phosphopeptides is more indicative of the conditions and environment found in a complex lysate or proteolytic digest and reinforces the need to carefully consider all experimental conditions when determining which phosphopeptide enrichment technique to use. The fact that peptides of all characteristics are recovered by CLIPP is highly encouraging, and the confirmation that this technique is also applicable to phosphotyrosine-containing peptides is a key feature of CLIPP. Further investigation into the workflow will be required to unravel the possible bias against basic, positively charged peptides that is seen in Table 2, as well as to apply this novel method to the global enrichment and identification of phosphosites in a complex sample.

Table 2. Overall pPep recovery yields for different workflow conditions.

Entry	pPep	I[a]	II[b]	III[c,d]
1	**pSer-2**	66±2%	69±2%	–
2	**pTyr-3**	34±2%	50±5%	37±2%
3	**pSer-4**	21±2%	29±6%	2±0%
4	**$(pSer)_2$-5**	30±8%	38±3%	0.2±0%
5	**pSer-6**	11±3%	12±2%[d]	18±2%

n=3 (triplicate) unless otherwise noted. [a] Original conditions (see Figure 4b). [b] Optimized enrichment conditions. [c] Enrichment yield from equimolar mixture of peptides (see Figure S5). [d] n=2 (duplicate).

Conclusion

Exploiting the remarkable efficiency and selectivity of phosphorimidazolide reagents, a new chemical modification strategy for phosphopeptide enrichment termed CLIPP has been developed. The use of btNPE-imidazolide **1** results in similar pyrophosphorylation efficiency compared to previous studies,[47,48] supporting its use in sequence with downstream immobilization, photoirradiation and hydrolysis. CLIPP displays reasonable efficiency compared to other chemical derivatization methods,[36] while exhibiting the capacity to modify a diverse set of peptides possessing highly variable characteristics. Acidic, basic, hydrophobic, phosphotyrosine, singly and doubly phosphorylated peptides were all modified and eluted with CLIPP following thorough characterization and optimization, and all four phosphopeptides were recovered when subjected to the CLIPP workflow in an equimolar mixture. Despite the capability of CLIPP to modify and enrich phosphopeptides with varying characteristics, there were distinct differences in overall yield. In particular, the yield for highly basic and acidic peptides were lower compared to the hydrophobic pTyr-containing **pTyr-3** when subjected to CLIPP in an equimolar mixture. To our knowledge, this paper represents the first quantification of relative bias between several phosphopeptides of specific characteristics for any method of chemical modification and elution of phosphopeptides. Previously, only PAC had reported a quantified enrichment of a defined phosphopeptide: an angiotensin-derived phosphopeptide enriched at a yield of ~40% from a BSA digest background using isotope labeling methods.[36] Further study of phosphopeptide enrichment with CLIPP will necessitate the application and optimization of CLIPP in complex samples containing both phospho- and non-phosphopeptides to be able to directly compare the utility of CLIPP to previously reported protocols.

The mild conditions employed throughout the workflow are a departure from existing methods that require the use of strongly acidic or basic conditions. The use of lanthanide(III) ions to hydrolyze pyrophosphate monoesters has not been previously reported, and their utility under conditions of mild pH and physiological temperature could result in the ability to enrich and annotate more labile modifications, such as phosphohistidine,[56] phosphocysteine,[57] or phospholysine,[58] modifications that have evaded comprehensive identification and characterization due to their labile nature and low

stoichiometry.[59] Future investigation of this unique hydrolysis reaction will focus on its applicability to synthetic standards of labile pyrophosphopeptides, with the hope of extending CLIPP into this emerging research area.

In sum, CLIPP takes advantage of the unique reactivity of phosphorimidazolide reagents towards phosphate monoesters, couples it to mild photoirradiation and lanthanide-mediated hydrolysis, resulting in a versatile methodology for the enrichment of diverse phosphopeptides. The approach holds great promise as a new and complementary method for the annotation of unique phosphorylation events throughout the phosphoproteome.

Experimental Section

HPLC analysis: For detailed HPLC methods and instrumentation, see Supporting Information.

General procedure for pyrophosphorylation of phosphopeptides with btNPE-imidazolide 1: For full details, see Supporting Information. 1 eq. of phosphopeptide and 3 eq. of **1** were dissolved in 100% dimethylacetamide (DMA) or 90%/10% DMA/H_2O containing 8 eq. $ZnCl_2$. Reactions were typically carried out with 1 mg or more of phosphopeptide, and at concentrations of at least 15 mM phosphopeptide. The resulting solution was incubated with stirring at 45 °C for 3 hours, or until complete (progress measured by LC–MS or analytical HPLC). Reaction was quenched with excess EDTA in water, and mixtures were analyzed *via* HPLC, LC–MS, or purified by preparative HPLC. For specific CLIPP pyrophosphorylation conditions, see below.

Immobilization of btNPE-ppSer-2, btNPE-ppTyr-3, btNPE-ppSer-4 and photoirradiation: 75 nmol GE High Performance streptavidin Sepharose resin (300 nmol/mL, never more than 75 nmol) was added to a 1 mL Pierce spin column and washed with 1.5 mL 1× PBS (20 mM phosphate, 150 mM NaCl, pH 7.5). For BSA pre-blocked resin, resin was incubated for 1 h in 1.0–1.5 mg/mL BSA (Carl Roth GmbH + Co. KG) in 1 × PBS), then washed with 1.5 mL 1× PBS. To the washed resin was added 250 μL of a 100 μM solution of btNPE-ppPep in 1× PBS containing 200 nmol $ZnCl_2$, 60 mM EDTA, 1.8% DMA. The spin column was sealed and agitated at room temperature for 30 min at 1200 rpm. The supernatant was then collected, and the resin washed 2× with 250 μL 1× PBS. The washes were combined with the immobilization supernatant and lyophilized for HPLC and/or LC–MS analysis to confirm immobilization. The resin was then further washed with 2.5 mL (5×500 μL) 20 mM HEPES pH 7.8. Following the final wash, the spin column was sealed, a micro-stirbar was added, and the resin suspended in 250 μL 20 mM HEPES pH 7.8. The suspension was then irradiated at 360 nm with an intensity of ~200 mW/cm^2 for 1 h at room temperature with vigorous stirring. Following irradiation, the supernatant was collected, and the resin washed 2× with 250 μL 20 mM HEPES pH 7.8. The irradiated supernatant was combined with the washes, 3.75 μL 500 mM EDTA was added, and the resulting solution was analyzed *via* LC–MS and/or HPLC (Method A, D, H) to confirm elution of ppSer-**2**, **ppTyr-3**, and ppSer-**4**.

Non-specific immobilization of pSer-2, pTyr-3, and pSer-4: 75 nmol of GE High Performance streptavidin Sepharose resin (300 nmol/mL, 3 eq. for each peptide phosphoryl group) was added to a 1 mL Pierce spin column and washed with 1.5 mL 1× PBS (20 mM phosphate, 150 mM NaCl, pH 7.5). For BSA pre-blocked resin, resin was incubated for 1 h in 1.0–1.5 mg/mL BSA, then washed with 1.5 mL PBS. To the washed resin was added 250 μL of a 1× PBS solution containing 25 nmol of pPep, 200 nmol $ZnCl_2$, 12 mM EDTA and 1.8% DMA. The spin column was sealed and agitated at room temperature for 30 min at 1200 rpm. The supernatant was then collected *via* centrifugation, the resin washed 2× with 250 μL PBS, and the combined supernatant and washes were submitted to analysis by HPLC for quantifying amount of phosphopeptide remaining in the supernatant.

In solution lanthanide hydrolysis of ppSer-2: 100 μL solutions containing 5 nmol **ppSer-2**, 20 mM HEPES pH 7.8 and the desired concentration of lanthanide ions (0, 50, 100, 250, or 500 μM) were incubated at the desired temperature for 18 h with 700 rpm agitation in an Eppendorf Thermomixer with an insulated lid. After 18 h the reactions were quenched with 1 μL 500 mM EDTA and analyzed by HPLC (HPLC method A). Hydrolysis was quantified with an HPLC standard curve of **pSer-2**, while a standard curve was used to confirm the starting amount of **ppSer-2** (see Supporting Information).

Solid-phase lanthanide hydrolysis of immobilized btNPE-ppSer-2: 10 nmol **btNPE-ppSer-2** was immobilized on 15 nmol of GE High Performance streptavidin Sepharose resin as previously described. Immobilized resin was washed with 1× PBS followed by 20 mM HEPES pH 7.8 as before, and the resin then suspended in 100 μL 20 mM HEPES pH 7.8 containing the desired concentration of lanthanide ions (0, 250, or 500 μM). The suspensions were then incubated at the desired temperature for 18 h with 1000 rpm agitation in an Eppendorf Thermomixer with an insulated lid. After 18 h 1 μL 500 mM EDTA was added to each suspension, and the supernatant collected. The resin was washed 2× with 50 μL 20 mM HEPES pH 7.8, and the washes were combined with the supernatant for analysis by HPLC (Method A). Elution was quantified *via* HPLC standard curve (see Supporting Information).

Chemoselective labeling, immobilization, elution and hydrolysis of pSer-2, pTyr-3, pSer-4, $(pSer)_2$-5, pSer-6: GE High Performance Streptavidin Sepharose Resin (75 nmol; 300 nmol/mL) was added to a 1 mL Pierce spin column and washed with 1.5 mL 1× PBS (20 mM phosphate, 150 mM NaCl, pH 7.5). For BSA pre-blocked resin, prepared as indicated above. Separately, 75 nmol of **1** was dissolved in 5 μL of a 9:1 DMA : water or 100% DMA solution containing 200 nmol $ZnCl_2$ for a final concentration of 15 mM **1**. This solution was sonicated to ensure that the phosphorimidazolide had fully dissolved, and the solution was then directly added to solid phosphopeptide. The resulting solution was heated at 45 °C for 3 h with 700 rpm agitation in an Eppendorf Thermomixer with an insulated lid. After 3 h, the reaction was quenched with 50 μL 60 mM EDTA and brought to a final volume of 250 μL with 170 μL ultrapure water and 25 μL 10× PBS (200 mM phosphate, 1.5 M NaCl). This quenched reaction solution was added directly to the washed resin, and the tube was sealed and agitated at room temperature for 30 min at 1200 rpm. The supernatant was then collected, and the resin washed 2× with 250 μL 1× PBS. The washes were combined with the immobilization supernatant and lyophilized for HPLC analysis to confirm complete removal of the phosphopeptides from solution. The resin was then further washed with 2.5 mL 20 mM HEPES pH 7.8. Following the final wash, the spin column was sealed, a micro-stirbar was added, and the resin suspended in 250 μL 20 mM HEPES pH 7.8. The tube was then sealed, and the suspension irradiated at 360 nm for 1 h at room temperature with vigorous stirring. Following irradiation, the irradiation supernatant was collected, and the resin washed 2× with 250 μL 20 mM HEPES pH 7.8. The irradiation supernatant was combined with the washes, 7.5 μL of a solution containing 10 mM of both $Lu(OTf)_3$ and $Y(OTf)_3$ was then added, and the lanthanide-containing solution was incubated for 18 h at 37 °C at 700 rpm in an Eppendorf Thermomixer with insulated lid. After 18 h, 2.5 μL 500 mM EDTA was added, and the resulting solution was analyzed

via LC–MS and HPLC. For peptides **pSer-6** and **$(pSer)_2$-5**, the hydrolysis reaction was lyophilized and then resuspended in 100 μL of ultrapure water before HPLC analysis. Recovery of pPep was quantified *via* the corresponding HPLC standard curve (using the same HPLC method - see Supporting Information). To track the yields of individual steps within a workflow, 60 μL aliquots were removed following photoirradiation and bead washing, and hydrolysis quenching. Aliquots analyzed by HPLC to determine the yields of intermediate steps.

^{31}P NMR stability studies of btNPE-imidazolide (1): btNPE-imidazolide (**1**) (2 mg; 2.08 μmol) was dissolved in 600 μL DMA and ^{31}P NMR spectrum detected as t = 0 min. 2.67 eq. $ZnCl_2$ were added as a 340 mM $ZnCl_2$ solution in DMA. NMR spectra were detected over a time span of 1165 min.

Chemoselective labeling, immobilization, elution, and hydrolysis of equimolar mixture of pTyr-3, pSer-4, $(pSer)_2$-5, pSer-6: Procedure was conducted identically to the CLIPP workflow of individual peptides (with BSA pre-blocked resin), except that ~5 nmol of each pPep were combined (20 nmol total phosphopeptide, 25 total nmol phosphoryl groups due to diphosphorylated **$(pSer)_2$-5**) and reacted with 75 nmol 1 for immobilization onto 75 nmol of BSA-blocked GE Sepharose high-performance streptavidin resin in both 9:1 DMA:H_2O and 100% DMA. The quenched hydrolysis solution was submitted to LC–MS analysis, and the ion chromatograms were extracted for the most abundant ions for each peptide in the mixture $[(M+3H)^{3+}/3]$.

Preparation of peptide HPLC standard curves: For each peptide, three 200 μL 1.25 mM solutions with concentration 0.625 or 1.25 mM were prepared in 20 mM HEPES pH 7.8 with 5 mM EDTA. From these solutions, 9 consecutive 2-fold serial dilutions were prepared for a total of 10 samples (lowest concentration 2.4 μM). Each sample was injected twice on the HPLC: 5 μL and 10 μL of sample 1 (1.25 mM) were injected, while 5 μL and at 30 μL of the 9 remaining samples were injected for a total of 20 injections per set of 10 samples. For the standard curve of **ppSer-2**, it was found that 50 mM citric acid (HPLC method A) was required for Buffer A in order to ensure consistent peak shape and retention time of **ppSer-2** (Figure S6). Therefore, both **pSer-2** and **ppSer-2** were run on an HPLC method containing 50 mM citric acid in buffer A. Chromatogram peak area was tabulate for each injection, and a linear regression performed in Microsoft Excel to calculate a linear fit (see Supporting Information for equations as well as HPLC methods used). Peak area of 274 nm absorbance was integrated for peptides **pSer-2**, **btNPE-ppSer-2** and **ppSer-2**, while 214 nm was used for all other peptides. Triplicate curves were used to calculate standard deviation of individual data points for all peptides except **btNPE-ppSer-2** due to sample availability. Peak areas that could not be detected for all three samples were omitted from the analysis. Prior to any reaction, 2–3 aliquots of the peptide(s) of interest were injected onto the analytical HPLC and the corresponding standard curve was used to calculate the peptide concentration for use in calculations of yield and necessary reagent.

Acknowledgements

The authors would like to acknowledge the MS facility, NMR facility and peptide facility of the FMP, as well as the entire Fiedler lab for their support and input. We would also like to acknowledge Lisa M. Yates for her groundwork on lanthanide hydrolysis. Open Access funding enabled and organized by Projekt DEAL.

Conflict of Interest

The authors declare no conflict of interest.

Data Availability Statement

The data that support the findings of this study are available from the corresponding author upon reasonable request.

Keywords: chemical biology · lanthanides · phosphopeptide · phosphorimidazolide · post-translational modifications

[1] S. J. Humphrey, D. E. James, M. Mann, *Trends Endocrinol. Metab.* **2015**, *26*, 676–687.
[2] F. Ardito, M. Giuliani, D. Perrone, G. Troiano, L. Lo Muzio, *Int. J. Mol. Med.* **2017**, *40*, 271–280.
[3] J. V. Olsen, B. Blagoev, F. Gnad, B. Macek, C. Kumar, P. Mortensen, M. Mann, *Cell* **2006**, *127*, 635–648.
[4] R. Aebersold, M. Mann, *Nature* **2003**, *422*, 198–207.
[5] J. Fíla, D. Honys, *Amino Acids* **2012**, *43*, 1025–47.
[6] I. L. Batalha, C. R. Lowe, A. C. A. Roque, *Trends Biotechnol.* **2012**, *30*, 100–10.
[7] C. Yang, X. Zhong, L. Li, *Electrophoresis* **2014**, *35*, 3418–3429.
[8] P. A. Grimsrud, D. L. Swaney, C. D. Wenger, N. A. Beauchene, J. J. Coon, *ACS Chem. Biol.* **2010**, *5*, 105–119.
[9] K. Engholm-Keller, M. R. Larsen, *Proteomics* **2013**, *13*, 910–931.
[10] M. P. Coghlan, T. S. Pillay, J. M. Tavaré, K. Siddle, *Biochem. J.* **1994**, *303*, 893–9.
[11] Q. P. Weng, M. Kozlowski, C. Belham, A. Zhang, M. J. Comb, J. Avruch, *J. Biol. Chem.* **1998**, *273*, 16621–9.
[12] H. Zhang, X. Zha, Y. Tan, P. V. Hornbeck, A. J. Mastrangelo, D. R. Alessi, R. D. Polakiewicz, M. J. Comb, *J. Biol. Chem.* **2002**, *277*, 39379–87.
[13] J.-M. Kee, R. C. Oslund, D. H. Perlman, T. W. Muir, *Nat. Chem. Biol.* **2013**, *9*, 416–21.
[14] J.-M. Kee, R. C. Oslund, A. D. Couvillon, T. W. Muir, *Org. Lett.* **2015**, *17*, 187–9.
[15] J. Fuhrmann, V. Subramanian, P. R. Thompson, *Angew. Chem.* **2015**, *127*, 14928–14931; *Angew. Chem. Int. Ed.* **2015**, *54*, 14715–14718.
[16] H. Ouyang, C. Fu, S. Fu, Z. Ji, Y. Sun, P. Deng, Y. Zhao, *Org. Biomol. Chem.* **2016**, *14*, 1925–1929.
[17] S. B. Ficarro, M. L. McCleland, P. T. Stukenberg, D. J. Burke, M. M. Ross, J. Shabanowitz, D. F. Hunt, F. M. White, *Nat. Biotechnol.* **2002**, *20*, 301–305.
[18] T. S. Nühse, A. Stensballe, O. N. Jensen, S. C. Peck, *Mol. Cell. Proteomics* **2003**, *2*, 1234–43.
[19] R. N. Joshi, N. A. Binai, F. Marabita, Z. Sui, A. Altman, A. J. R. Heck, J. Tegnér, A. Schmidt, *Front. Immunol.* **2017**, *8*, 1163.
[20] M. Gridling, S. B. Ficarro, F. P. Breitwieser, L. Song, K. Parapatics, J. Colinge, E. B. Haura, J. A. Marto, G. Superti-Furga, K. L. Bennett, U. Rix, *Mol. Cancer Ther.* **2014**, *13*, 2751–62.
[21] M. R. Larsen, T. E. Thingholm, O. N. Jensen, P. Roepstorff, T. J. D. Jørgensen, *Mol. Cell. Proteomics* **2005**, *4*, 873–886.
[22] Y. Oda, T. Nagasu, B. T. Chait, *Nat. Biotechnol.* **2001**, *19*, 379–382.
[23] P. van der Veken, E. H. C. Dirksen, E. Ruijter, R. C. Elgersma, A. J. R. Heck, D. T. S. Rijkers, M. Slijper, R. M. J. Liskamp, *ChemBioChem* **2005**, *6*, 2271–2280.
[24] D. T. McLachlin, B. T. Chait, *Anal. Chem.* **2003**, *75*, 6826–6836.
[25] S. M. Stevens, A. Y. Chung, M. C. Chow, S. H. McClung, C. N. Strachan, A. C. Harmon, N. D. Denslow, L. Prokai, *Rapid Commun. Mass Spectrom.* **2005**, *19*, 2157–2162.
[26] C. Klemm, S. Schröder, M. Glückmann, M. Beyermann, E. Krause, *Rapid Commun. Mass Spectrom.* **2004**, *18*, 2697–2705.
[27] G. Arrigoni, S. Resjö, F. Levander, R. Nilsson, E. Degerman, M. Quadroni, L. A. Pinna, P. James, *Proteomics* **2006**, *6*, 757–766.
[28] K. Vosseller, K. C. Hansen, R. J. Chalkley, J. C. Trinidad, L. Wells, G. W. Hart, A. L. Burlingame, *Proteomics* **2005**, *5*, 388–398.
[29] Z. A. Knight, B. Schilling, R. H. Row, D. M. Kenski, B. W. Gibson, K. M. Shokat, *Nat. Biotechnol.* **2003**, *21*, 1047–1054.
[30] F. Rusnak, J. Zhou, G. M. Hathaway, *J. Biomol. Tech.* **2002**, *13*, 228–37.

[31] H.-C. Tseng, H. Ovaa, N. J. C. Wei, H. Ploegh, L.-H. Tsai, *Chem. Biol.* **2005**, *12*, 769–777.
[32] K. D. Green, M. K. H. Pflum, *J. Am. Chem. Soc.* **2007**, *129*, 10–11.
[33] C. Senevirathne, D. M. Embogama, T. A. Anthony, A. E. Fouda, M. K. H. Pflum, *Bioorg. Med. Chem.* **2016**, *24*, 12–19.
[34] H. Zhou, J. D. Watts, R. Aebersold, *Nat. Biotechnol.* **2001**, *19*, 375–378.
[35] W. A. Tao, B. Wollscheid, R. O'Brien, J. K. Eng, X. Li, B. Bodenmiller, J. D. Watts, L. Hood, R. Aebersold, *Nat. Methods* **2005**, *2*, 591–8.
[36] B. Bodenmiller, L. N. Mueller, P. G. A. Pedrioli, D. Pflieger, M. A. Jünger, J. K. Eng, R. Aebersold, W. A. Tao, *Mol. BioSyst.* **2007**, *3*, 275.
[37] M. Warthaka, P. Karwowska-Desaulniers, M. Kay, H. Pflum, *ACS Chem. Biol.* **2006**, *1*, 697–701.
[38] B. Bodenmiller, L. N. Mueller, M. Mueller, B. Domon, R. Aebersold, *Nat. Methods* **2007**, *4*, 231–237.
[39] B. Lombardi, N. Rendell, M. Edwards, M. Katan, J. G. Zimmermann, *EuPA Open Proteomics* **2015**, *6*, 10–15.
[40] X. Yue, A. Schunter, A. B. Hummon, *Anal. Chem.* **2015**, *87*, 8837–44.
[41] R. Lohrmann, L. E. Orgel, *Science* **1968**, *161*, 64–66.
[42] B. J. Weimann, R. Lohrmann, L. E. Orgel, H. Schneider-Bernloehr, J. E. Sulston, *Science* **1968**, *161*, 387.
[43] M. Shimazu, K. Shinozuka, H. Sawai, *Tetrahedron Lett.* **1990**, *31*, 235–238.
[44] M. Kadokura, T. Wada, C. Urashima, M. Sekine, *Tetrahedron Lett.* **1997**, *38*, 8359–8362.
[45] B. C. F. Chu, L. E. Orgel, *Biochim. Biophys. Acta Gene Struct. Expression* **1984**, *782*, 103–105.
[46] M. Strenkowska, P. Wanat, M. Ziemniak, J. Jemielity, J. Kowalska, *Org. Lett.* **2012**, *14*, 4782–5.
[47] A. M. Marmelstein, L. M. Yates, J. H. Conway, D. Fiedler, *J. Am. Chem. Soc.* **2014**, *136*, 108–111.
[48] A. M. Marmelstein, J. A. M. Morgan, M. Penkert, D. T. Rogerson, J. W. Chin, E. Krause, D. Fiedler, *Chem. Sci.* **2018**, *9*, 5929–5936.
[49] M. Penkert, L. M. Yates, M. Schümann, D. Perlman, D. Fiedler, E. Krause, *Anal. Chem.* **2017**, *89*, 3672–3680.
[50] S. J. Franklin, *Curr. Opin. Chem. Biol.* **2001**, *5*, 201–8.
[51] S. Hashimoto, Y. Nakamura, *J. Chem. Soc. Perkin Trans. 1* **1996**, 2623.
[52] M. Komiyama, *J. Biochem.* **1995**, *118*, 665–70.
[53] S. Cotton, *Lanthanide and Actinide Chemistry*, Wiley, **2006**.
[54] V. Mayya, D. H. Lundgren, S.-I. Hwang, K. Rezaul, L. Wu, J. K. Eng, V. Rodionov, D. K. Han, *Sci. Signaling* **2009**, *2*, ra46.
[55] J. V. Olsen, M. Vermeulen, A. Santamaria, C. Kumar, M. L. Miller, L. J. Jensen, F. Gnad, J. Cox, T. S. Jensen, E. A. Nigg, S. Brunak, M. Mann, *Sci. Signaling* **2010**, *3*, ra3.
[56] C. M. Potel, M.-H. Lin, A. J. R. Heck, S. Lemeer, *Nat. Methods* **2018**, *15*, 187–190.
[57] J. Bertran-Vicente, M. Penkert, O. Nieto-Garcia, J.-M. Jeckelmann, P. Schmieder, E. Krause, C. P. R. Hackenberger, *Nat. Commun.* **2016**, *7*, 12703.
[58] J. Bertran-Vicente, R. A. Serwa, M. Schümann, P. Schmieder, E. Krause, C. P. R. Hackenberger, *J. Am. Chem. Soc.* **2014**, *136*, 13622–13628.
[59] A. M. Marmelstein, J. Moreno, D. Fiedler, *Top. Curr. Chem.* **2017**, *375*, 22.

Manuscript received: July 19, 2022
Revised manuscript received: September 21, 2022
Accepted manuscript online: September 27, 2022
Version of record online: October 26, 2022